Jurnal Penyelidikan dan Pendidikan Kejuruteraan. Jilid 1, 2004

Feature Extraction of Trademark Images Using Geometric Invariant Moment and Zernike Moment – A Comparison

PUTEH SAAD, NURSALASAWATI RUSLI
School of Computer & Communication Engineering,
Kolej Universiti Kejuruteraan Utara Malaysia(KUKUM), Blok A, Kompleks Pusat Pengajian,
Jalan Kangar-Arau,02600 Jejawi, Perlis, MALAYSIA.

ABSTRACT

The qualities of features extracted determine the successfulness of any image related applications. This is particularly true especially when the natures of images are occluded and consist of various shapes and design styles, such as trademark images. In this study Geometric Invariant Moment and Zernike Moment techniques are utilized to extract sets of features from trademark images. The results obtained are analysed and compared in terms of intraclass invariance to various perturbations. It is found that a set of features produced by Zernike Moment technique is more robust when compared to features produced by Geometric Invariant Moment.

INTRODUCTION

Feature Extraction is crucially significant for the successfulness of the image-related applications [1][2][3][4][5][6]. It is still a dream for the computer to outperform human natural ability for visual interpretation, thus feature extraction still remains a challenging task in various realms of computer vision and image analysis.

Monochrome or one colour (black and white) trademark images belong to the category of silhouette image, where shape attribute is normally used to represent the image content. Moment-based techniques are chosen to perform the feature extraction due to the following reasons [7].

- a set of moments computed from a digital image represent global characteristics of the image shape,
- it also provides a lot of information regarding the different types of geometrical features inherent in the image and
- it produces a set of features that is invariant

The paper starts by describing the Geometric invariant moment technique in Section 2, Zernike moment technique in Section 3. Section 4 presents the implementation, Section 5 highlight Results and Discussion. The paper ends with a conclusion in Section 6.

METHODOLOGY

Geometric invariant moment techniques

Geometric invariant moment technique is chosen to extract image features since the features generated are Rotation Scale Translation (RST)-invariant. Geometric Moment Invariant was first introduced by Hu and it is also known in some literature as Hu's Moment Invariants [8]. This moment was derived from the theory of algebraic invariant. Geometric Moment was successfully applied in aircraft identification, texture classification and radar images to optical images matching [9]. The properties of geometrical Moment has the form of a projection of the $f(x,y)$ function onto the monomial $x^p y^q$. Properties of Geometric Moment as as follows;

For a 2-D continuous function $f(x,y)$, the moment of order (p+q) is defined as

$$m_{pq} = \int_{-\infty}^{\infty}\int_{-\infty}^{\infty} x^p y^q f(x,y)dxdy \qquad (1.1)$$

for $p,q = 0,1,2,3,\ldots$

A unique theorem [8] states that if $f(x,y)$ is piecewise continuous and has nonzero values only in a finite part of the xy plane, moment of all orders exist and the moment sequence m_{pq} is uniquely determined by $f(x,y)$. Conversely, m_{pq} uniquely determines $f(x,y)$. The central moments can be expressed as

$$\mu_{pq} = \int_{-\infty}^{\infty}\int_{-\infty}^{\infty} (x-\bar{x})^p (y-\bar{y})^q f(x,y) \qquad (1.2)$$

where

$$\bar{x} = \frac{m_{10}}{m_{00}} \quad \text{and} \quad \bar{y} = \frac{m_{01}}{m_{00}}$$

$$\mu_{pq} = \sum_x \sum_y (x-\bar{x})^p (y-\bar{y})^q f(x,y) \qquad (1.3)$$

For a grey scale image, Equation (1.2) becomes
For binary digital image, $f(x,y) = 1$ (indicating an object), thus Equation (1.3) becomes

$$\mu_{pq} = \sum_x \sum_y (x-\bar{x})^p (y-\bar{y})^q \qquad (1.4)$$

The centralised moments μ_{pq} can be expressed in terms of m_{pq} as follows:

$$\left.\begin{aligned}
\mu_{00} &= m_{00} \\
\mu_{10} &= 0 \\
\mu_{01} &= 0 \\
\mu_{20} &= m_{20} - xm_{10} \\
\mu_{02} &= m_{02} - ym_{01} \\
\mu_{11} &= m_{11} - ym_{10} \\
\mu_{31} &= m_{30} - 3xm_{20} + 2xm_{10} \\
\mu_{12} &= m_{12} - 2ym_{11} - xm_{02} + 2ym_{10} \\
\mu_{21} &= m_{21} - 2xm_{11} - ym_{20} + 2xm_{01} \\
\mu_{03} &= m_{03} - 3ym_{02} + 2ym_{01}
\end{aligned}\right\} \quad (1.5)$$

The normalized central moments are defined as;

$$\eta_{pq} = \frac{\mu_{pq}}{\mu_{00}^{\gamma}},$$

where,

$$\gamma = \frac{(p+q)}{2} + 1,$$

for (p+q) = 2, 3,...

The resulting moment functions which are taken as representative features of the image as shown below are invariant with respect to translation rotation and scale change [8].

$$\phi_1 = \eta_{20} + \eta_{02} \quad (1.6)$$

$$\phi_2 = (\eta_{20} - \eta_{02})^2 + 4\eta_{11}^2$$

$$\phi_3 = (\eta_{30} - 3\eta_{12})^2 + (3\eta_{21} - \eta_{03})^2$$

$$\phi_4 = (\eta_{30} + \eta_{12})^2 + (\eta_{21} + \eta_{03})^2$$

$$\phi_5 = (\eta_{30} - 3\eta_{12})(\eta_{30} + \eta_{12})[(\eta_{30} + \eta_{12})^2 - 3(\eta_{21} + \eta_{03})^2] + (3\eta_{21} - \eta_{03})(\eta_{21} + \eta_{03})[3(\eta_{30} + \eta_{12})^2 - (\eta_{21} + \eta_{03})^2]$$

$$\phi_6 = (\eta_{20} - \eta_{02})[(\eta_{30} + \eta_{12})^2 - (\eta_{21} + \eta_{03})^2] + 4\eta_{11}(\eta_{30} + \eta_{12})(\eta_{21} + \eta_{03})$$

$$\phi_7 = (3\eta_{21} - \eta_{30})(\eta_{30} + \eta_{12})[(\eta_{30} + \eta_{12})^2 - 3(\eta_{21} + \eta_{30})^2] + (3\eta_{12} - \eta_{30})(\eta_{21} + \eta_{03})[3(\eta_{30} + \eta_{12})^2 - (\eta_{21} + \eta_{03})^2]$$

Zernike moment technique

Zernike Moment (Z.M) is chosen since it is invariant to rotation and insensitive to noise. Another advantage of Z.M is the ease of image reconstruction because of its orthogonal

property [9][10][11][12][13]. Z.M is the projection of the image function onto orthogonal basis functions. Z.M also has a useful rotation invariance property where the magnitude of Z.M will not change for a rotated image. Another main property of Z.M is the ease of image reconstruction because of its orthogonal property [9]. The major drawback of Z.M is it's computational complexity [7]. This is due to the recursive computation of Radial Polynomials. However in this study, we overcome the problem of computational complexity by adopting a non recursive computation of Radial Polynomials. The computation is based on the relationship between Geometric Moment Invariant and Z.M in order to derive Zernike Invariant Moment. Properties of Z.M are as follows:

The Z.M of order p with repetition q for a continuos image function $f(x,y)$ that vanishes outside the unit circle is as shown in Eq. 1.9.

$$Z_{pq} = \frac{p+1}{\pi} \iint_{x^2+y^2=1} f(r,\theta) V^*_{pq} r dr d\theta \tag{1.9}$$

To compute a Z.M of a given image, the center of the image is taken as the origin and pixel coordinates are mapped to the range of unit circle, i.e. $x^2 + y^2 = 1$. The functions of $V_{pq}(r, \theta)$ denote Zernike Polynomials of order p with repetition q, and * denotes a complex conjugate where the Zernike Polynomials are defined as functions of the polar coordinates r, θ [6]. Equations relating Zernike and Geometric Moment up to third order are given below

$$\begin{aligned}
Z_{oo} &= (1/\pi)\, M_{oo} \\
Z_{11} &= (2/\pi)\,(M_{10} - i\, M_{01}) \\
Z_{20} &= (6/\pi)\,(M_{20} + M_{02}) - (3/\pi)\, M_{00} \\
Z_{22} &= (3/\pi)\,(M_{20} - M_{02} - 2i\, M_{11}) \\
Z_{31} &= (12/\pi)\,(M_{30} + M_{12}) - (12/\pi)i\,(M_{03} + M_{21}) - (8/\pi)\,(M_{10} - iM_{01}) \\
Z_{33} &= (4/\pi)\,(M_{30} - 3M_{12}) + (4/\pi)i\,(M_{03} - 3M_{21})
\end{aligned} \tag{1.10}$$

Rotation Invariants properties are illustrated as follows; from the definition of Z.M in Eq (1.9), when image undergoes a rotation by an angle α, the transformed moment functions Z'_{pq} are given by

$$Z'_{pq} = Z_{pq}\, e^{-iq\alpha} \tag{1.11}$$

This simple property leads to the conclusion that the magnitudes of the Z.M of a rotated image function remain identical to those before rotation. Thus $|Z_{pq}|$, the magnitude of the Z.M, can be taken as a rotation invariant feature of the underlying image function. Rotation invariants and their corresponding expressions in Geometric Moment (G.M)are given below until the order of three:

$$\left.\begin{aligned}
Z_{oo} &= (1/\pi)\, M_{oo} \\
|Z_{11}|^2 &= (2/\pi)^2\,(M_{10}^2 + M_{01}^2) \\
Z_{20} &= (3/\pi)\,[2M_{20} + M_{02}) - M_{00}] \\
|Z_{22}|^2 &= (3/\pi)^2\,[(M_{20} - M_{02})^2 + 4\, M_{11}^2) \\
|Z_{31}|^2 &= (12/\pi)^2\,[(M_{30} + M_{12})^2 + (M_{03} + M_{21})^2] \\
|Z_{33}|^2 &= (4/\pi)^2\,[(M_{30} - 3M_{12})^2 + (M_{03} - 3M_{21})^2]
\end{aligned}\right\} \tag{1.12}$$

Implementation

Monochrome image samples are obtained from Trademark Ordinance are scanned using 200 dpi HP Laser and Lexmark Scanner [14][15]. The scanned image is then saved as *.tiff* format. The image is then converted into gray-level format; the noise is removed and it is thresholded using Otsu thresholding algorithm [16], and then it is saved using the *raw* format. Before the image file is closed, its width and height in pixels are noted, since the dimensions will become an input to the feature extraction phase. The trademark image samples utilized in this endeavor as shown in Appendix A, are divided into four categories based on image shape;

Category 1	Circle
Category 2	Rectangle
Category 3	Word-Embedded Mark
Category 4	Miscellaneous

Due to the analysis and observation of the trademark image samples, majority of them fall under the above shape categories. Furthermore, based on the literature study conducted, the moment-based feature extraction techniques performed well in extracting the global image shape [17]. We want to find out the invariance property displayed by G.M and Z.M features of different trademark image shapes.

The image samples are perturbed to produce seven variants as depicted in Figure 1.1, and to test the robustness of the feature extraction techniques adopted.

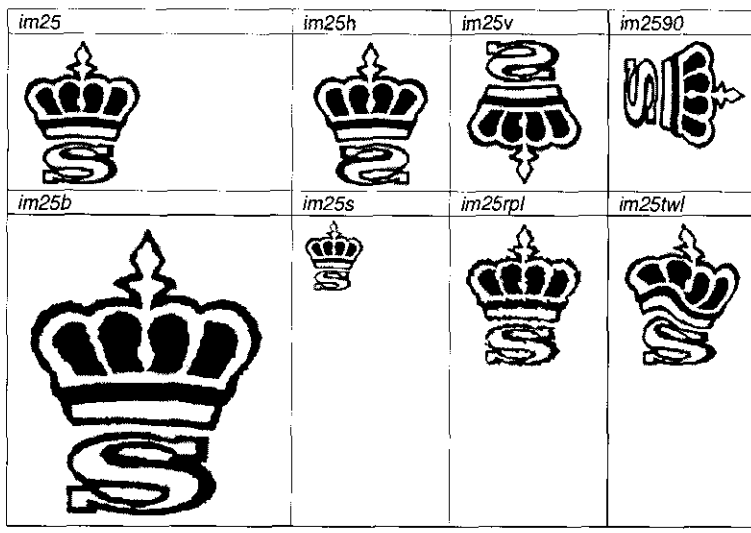

Figure 1: An Image Example (Image im25 and its variations)

The legend of the image variations is as follows:

im25	an original image
im25h	the original image placed horizontally
im25v	the original image placed vertically
im2590	the original image rotated to 90 degrees
im25b	the original image is enlarged by 50%
im25s	the original image is reduced by 50%
im25rpl	the original image is rippled to –160 degrees
im25twl	the original image twirled to –72 degrees

RESULTS AND DISCUSSION

A set of G.M and a set of Z.M features are extracted from image samples using Equation (1.6) and (1.12). Table 1, depicts an example of G.M Features Vectors of an original image and its variants belong to category 4. Table 2, depicts the Z.M features vectors of the same image.

Table 1: The G.M Feature Vector of Image im25 and its Variants

Variants	φ_1	φ_2	φ_3	φ_4	φ_5	φ_6	φ_7
im25	13.125976	24.450977	22.968588	23.027691	45.730889	0.000000	45.277840
im25h	13.134906	24.493625	22.896047	23.004788	34.542001	0.000000	0.000000
im25v	13.135990	24.506779	22.954658	22.998057	45.992919	0.000000	43.882536
im2590	13.874312	27.195126	27.565035	26.789870	53.638658	39.944855	0.000000
im25b	13.018402	23.274206	19.741464	18.195952	45.607242	0.000000	45.411974
im25s	13.133874	24.497487	22.764208	23.147620	43.820398	0.000000	43.095920
im25rpl	13.889930	25.967766	24.311989	24.510164	0.000000	35.117641	0.000000
im25twl	12.828828	23.837837	22.429150	21.836985	48.860318	0.000000	0.000000

Table 2: The Z.M Feature Vector of Image im25 and its Variants

Variants	φ_1	φ_2	φ_3	φ_4	φ_5	φ_6
im25	0	0	0.857123	0.000158	0.000165	0.000012
im25h	0	0	0.85405	0.000169	0.000172	0.000009
im25v	0	0	0.947745	0.003843	0.00005	0.000002
im2590	0	0	0.842004	0.023164	0.014305	0.007447
im25b	0	0	0.797769	0.00013	0.000007	0
im25s	0	0	0.782225	0.00011	0.000011	0.000005
im25rpl	0	0	0.806016	0.000101	0.000018	0.000002
im25twl	0	0	0.799257	0.000139	0.000032	0.000004

It is observed that Z.M orders 1 and 2 have null values and order 3 is significant. However with regard to G.M, higher order moment values of 4th and sometimes 5th and above tend to become insignificant.

Studies are performed to determine the sensitivity of Geometric Moment and Z.M techniques to various perturbations of each image selected from each image category. Based on *Equation 1.13, mean error($m\_e_{G.M}$) for G.M is computed for each image variants to determine* the intraclass invariances. Mean error is computed by first obtaining the absolute difference

between the original and the perturbed image for each moment function value, represented by $e_i(G.M)$.

$$e_i(G.M) = |\varphi_i(\text{original}) - \varphi_i(\text{perturbed})| \qquad i = 1,2,3,\ldots,6$$

$$m\_e_{G.M} = \frac{\sum_{i=1}^{i=6} e_i(G.M)}{6} \tag{1.13}$$

Table 3 depicts the values of the mean error of the G.M computed for an image belongs to Category 2.

Table 3: Mean Error of the G.M for an Image belongs to Category 2

	φ_1	φ_2	φ_3	φ_4	φ_5	φ_6	φ_7
im2	11.53581	15.68733	21.30834	21.46877	42.85977	29.13757	0
im2h	11.53545	15.32017	21.38324	21.43602	42.84385	29.0807	0
Error	0.000347	0.367167	0.074903	0.032751	0.015921	0.056871	
Mean error	**0.09133**						
im2	11.53581	15.68733	21.30834	21.46877	42.85977	29.13757	0
im2v	11.53627	15.44956	21.418	21.42433	42.84469	29.02954	38.95749
Error	0.00064	0.23777	0.109659	0.044443	0.01508	0.108028	
Mean error	**0.08594**						
im2	11.53581	15.68733	21.30834	21.46877	42.85977	29.13757	0
im290	11.58467	21.52448	17.68996	14.592	25.3782	25.28261	0
Error	0.048859	5.837147	3.618376	6.876768	17.48157	3.854962	
Mean error	**6.28628**						
im2	11.53581	15.68733	21.30834	21.46877	42.85977	29.13757	0
im2b	12.73269	20.14596	23.1244	23.21481	46.38438	33.28769	41.49746
Error	1.196879	4.458631	1.816058	1.746038	3.524612	4.150117	
Mean error	**2.81539**						
im2	11.53581	15.68733	21.30834	21.46877	42.85977	29.13757	0
im2s	11.04624	16.48165	18.9925	19.26641	38.38296	27.47657	35.90499
Error	0.489567	0.794321	2.315839	2.202358	4.47681	1.661006	
Mean error	**1.989984**						
im2	11.53581	15.68733	21.30834	21.46877	42.85977	29.13757	0
im2rpl	11.63838	18.10983	20.59558	20.64279	41.26226	29.67897	37.34499
Error	0.102568	2.422501	0.712762	0.825981	1.59509	0.541402	
Mean error	**1.033384**						
im2	11.53581	15.68733	21.30834	21.46877	42.85977	29.13757	0
im2twl	11.61208	17.61469	20.914	20.48733	41.1649	29.2849	0
Error	0.102568	1.927353	0.394337	0.981438	1.694863	0.147332	
Mean error	**0.87465**						

Similarly as for Z.M, absolute difference between original and perturbed image is first computed, then followed by getting the mean error($m\_e_{Z.M}$) using Equation 1.14.

$$e_i(ZM) = |\varphi_i(\text{original}) - \varphi_i(\text{perturbed})| \; i = 3, 4, \ldots, 6$$

$$m\_e_{Z.M} = \frac{\sum_{i=3}^{i=6} e_i(Z.M)}{4} \tag{1.14}$$

Table 4 : depicts the values of the mean error of the Z.M computed for the same image.

Table 4: Mean Error of the Z.M of an image belongs to Category 2

	φ_1	φ_2	φ_3	φ_4	φ_5	φ_6
im2	0	0	0.613385	0.009635	0.01039	0.001653
im2h	0	0	0.616112	0.009891	0.010391	0.00168
error	0	0	0.002727	0.000256	0.000001	0.0000026
mean error	**0.000747**					
im2	0	0	0.613385	0.009635	0.01039	0.001653
im2v	0	0	0.695523	0.012745	0.021135	0.002812
error	0	0	0.082138	0.00311	0.00311	0.001159
mean error	**0.022379**					
im2	0	0	0.613385	0.009635	0.01039	0.001653
im290	0	0	0.664766	0.005132	0.001403	0.000099
error	0	0	0.051381	0.004503	0.008987	0.001554
mean error	**0.016606**					
im2	0	0	0.613385	0.009635	0.01039	0.001653
im2b	0	0	0.571565	0.007125	0.005132	0.000644
error	0	0	0.04182	0.00251	0.005258	0.001009
mean error	**0.012649**					
im2	0	0	0.613385	0.009635	0.01039	0.001653
im2s	0	0	0.566212	0.006901	0.004786	0.000614
error	0	0	0.047173	0.002734	0.005604	0.001039
mean error	**0.014138**					
im2	0	0	0.613385	0.009635	0.01039	0.001653
im2rpl	0	0	0.56861	0.00706	0.005056	0.000645
error	0	0	0.044775	0.002575	0.005334	0.001008
mean error	**0.013423**					
im2	0	0	0.613385	0.009635	0.01039	0.001653
im2twl	0	0	0.569924	0.00741	0.005256	0.000815
error	0	0	0.043461	0.002225	0.005134	0.000838
mean error	**0.012915**					

In order to view the sensitivity of G.M and Z.M against various image orientations for different image categories graphs of mean error versus image variants for G.M and Z.M are plotted to further highlight the major differences, as depicted in **Figure 2** and **3.**

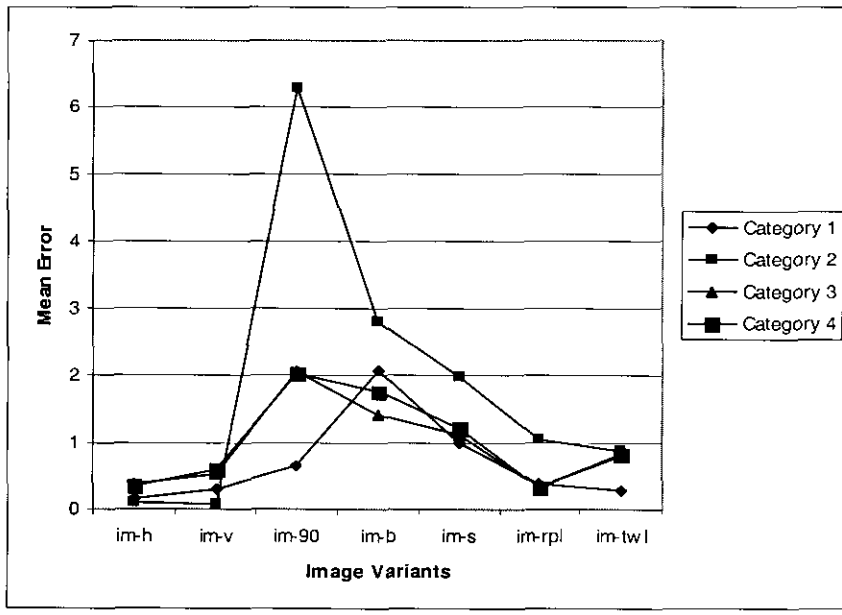

Figure 2: Graph of Mean Error vs. Image Variants of Different Categories for G.M

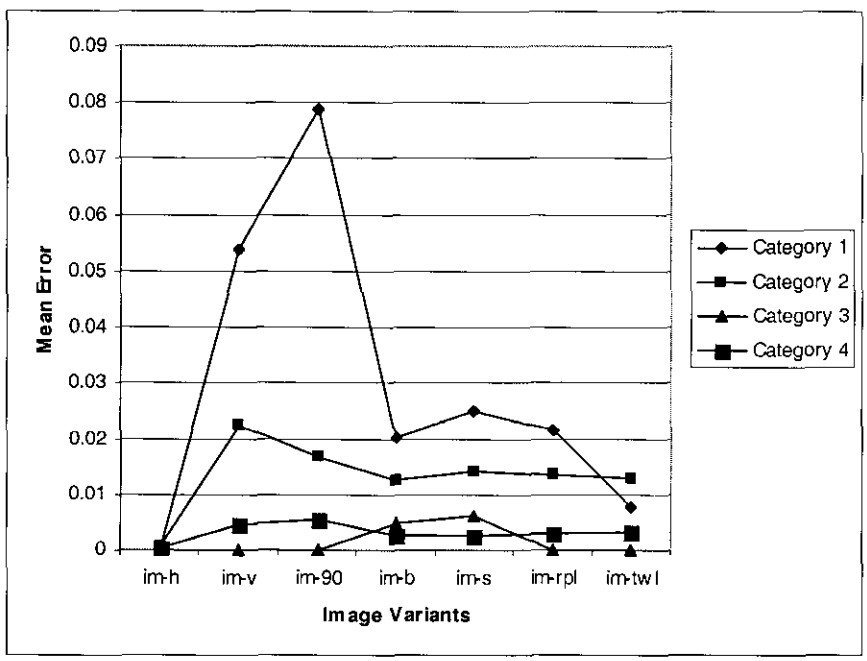

Figure 3: Graph of Mean Error vs. Image Variants of Different Categories for Z.M

Further analysis is done to determine intraclass invariances of each image category to different perturbations both for G.M and Z.M. Results are tabulated in Table 5 and 6.

Table 5: Intraclass invariances of G.M

Cat.	*Shape*	*im_h*	*im_v*	*imo_90*	*im_b*	*im_s*	*im_rpl*	*im_twl*
1	Circle	×	×	×	✓	×	×	×
2	Rectangle	×	×	✓✓	✓✓	✓✓	×	×
3	Word-embedded	×	×	✓	✓	×	×	×
4	Miscellaneous	×	×	✓	✓	×	×	×

where

Cat.	represents Category
im_h	the original image placed horizontally
im_v	the original image placed vertically
imo_90	the original image rotated to 90 degrees
im_b	the original image is enlarged by 50%
im_s	the original image is reduced by 50%
im_rpl	the original image is rippled to –160 degrees
im_twl	the original image twirled to –72 degrees
×	less sensitive (mean error below 1)
✓	slightly sensitive (1=<mean error <= 2)
✓✓	very sensitive (mean error > 3)

Similarly, in order to determine intraclass invariances of set of features produced by Z.M for each image category to each perturbation, analysis is further carried out on Figure 3 and the results are tabulated as shown in Table 6. Please note again here that the mean error range for Z.M falls below 0.1, very much lower than G.M.

Table 6: Intraclass invariances of Z.M

Cat.	*Shape*	*im_h*	*im_v*	*imo_90*	*im_b*	*im_s*	*im_rpl*	*im_twl*
1	Circle	×	✓✓	✓✓	✓	✓	✓	×
2	Rectangle	×	✓	×	×	×	×	×
3	Word-embedded	×	×	×	×	×	×	×
4	Miscellaneous	×	×	×	×	×	×	×

where

×	less sensitive (mean error < 0.01)
✓	moderately sensitive (0.01 =<mean error <=0.02)
✓✓	sensitive (0.02 =< mean error < 0.8)

Based on the sensitivity results portrayed in Table 5, the findings obtained regarding the set of G.M of trademark image features are as follows:

- It is invariant to horizontal, vertical, rippled and twirled perturbations for all trademark image categories.

- It is sensitive to image enlargement for all categories.
- 3 out of 4 categories are sensitive to image orientation.
- Category 2 (rectangle) is sensitive to orientation, size enlargement and size reduction.
- Category 1 (circle) is only sensitive to image enlargement.

Based on the sensitivity results portrayed in Table 6, it is found that the set of features produced by Z.M:

- all categories of trademark images are invariance to horizontal and twirled perturbations.
- trademark images belong to Category 2 (rectangle) are only sensitive to vertical perturbation.
- trademark images belong to Category 1 (circle) are sensitive to vertical and 90 angular orientation. They are moderately sensitive to image enlargement, image reduction and rippled perturbation.
- Trademark images belong to Category 3 and 4 are invariance to all perturbations.

It is noticed that set of G.M features for Category 2 (rectangle) is very sensitive to every image perturbations, however its Z.M features are invariant almost to all perturbations. On the other hand set of G.M features for Category 1 (circle) is almost invariant to all perturbations, however its Z.M features is sensitive to almost all perturbations.

The total moment functions of G.M obtained from central moments up to order three is seven. However it is observed that the values for higher-order moment functions from Moment Function 5 to Moment Function 7 are less significant when compared to lower-order moments. This is due to the intrinsic nature of trademark images that do not have a uniform distribution of black pixels due to occlusion, unlike hand-written numerals. In handwritten numerals, higher-order moment functions are significant [18]. On the other hand, Z.M has a total moment functions of six. Conversely, the lower-order moment functions of Z.M do not contribute at all to represent an image. Moments of order three is very significant and it becomes less significant as the moments orders are greater than three. This is due to computation of Z.M that is based on polar coordinates that constrained the image to a unit circle.

Studies are then performed to study the sensitivity of various image perturbations to both G.M and Z.M features. It is noticed that G.M is sensitive to image scaling with regard to size enlargement and 90 degree angular orientation. As for other perturbations like horizontal and vertical displacement, rippled and twirled, the G.M features are invariant. Images belong to Category 2 (rectangle) display the highest mean error in terms of size enlargement, size reduction and 90 degree angular orientation when compared to other shapes. The fact that the image is sensitive to 90 degrees angular orientation is because the G.M features are not rotation invariant, except for circle shape. Image of size circle is invariant to 90 degrees angular orientation is due to the nature of shape circle that maintain its original shape regardless of any rotation. With regards to scaling, when the trademark image undergoes perturbations, its global shape changes dramatically thus the G.M features differ too, since the G.M technique captures global shape. This finding falsifies the claim made by [8] in deriving the equations for a set of 7 moment functions.

The introduction of a parameter

$$\eta_{pq} = \frac{\mu_{pq}}{\mu_{00}^{\gamma}},$$

is insufficient to make the G.M features invariant to size for the case of trademark images. Hu tested the G.M invariance property on character recognition. Hence the size invariance is dependent on types of images used.

The mean errors of all image categories for Z.M features lie below 0.1, very much lower when compared to G.M features. Within the (0 to 0.08) range trademark images of shape circle and rectangle are sensitive to perturbations. Almost all perturbations affect trademark images of shape circle except horizontal displacement. This is due to the Z.M that are defined in terms of polar coordinates (r,θ), the Zernike polynomials will have to be evaluated at each pixel position. The polar form suggests a square-to-circular image transformation, so that the Zernike polynomials need to be computed only once for all pixels mapped to the same circle [7]. As for the image of type circle, it is possible the pixel coordinates (represented by the radius and position index of the pixel) of the transformed circular image differ from the original image that causes the variances observed.

Z.M image features belonging Category 3 and 4 are invariant to all perturbations. Category 3 is word-embedded mark. From the literature, it is found that Z.M has been successfully applied to extract features from handwritten numerals and alphabets [9][10][11][12][13]. However this is the first attempt of using Z.M function orders computed from G.M to extract features from trademark images. The results for intraclass variation are far better than G.M image features.

CONCLUSION

This paper presents G.M and Z.M as feature extraction techniques for trademark images, their implementations, results and evaluations of the resulting features in terms of scale, angular, position and distortion invariances. The findings obtained are that the set of trademark image features produced by G.M are invariant to position and distortion. It is sensitive to scale and 90 degrees angular orientation. However the Z.M features are invariant to all perturbations in this experiment, except for circle shape, however the mean error is acceptable (i.e. 0.08). Thus we can conclude that the set of features produced by Zernike Moment is of better quality than that of Geometric Invariant Moment technique.

REFERENCES

1. Gonzalez, R.C. and Woods, R.E, (1992). *Digital Image Processing.* Massachusetts: AddisonWesley Publication.

2. Umbaugh, S.E, (1998). *Computer Vision and Image Processing.* Upper Saddle River, New Jersey : Prentice-Hall International, Inc.

3. Sing, T.B, (1992). *Pattern Recognition and Image Pre-processing.* New York : Marcel Dekker, Inc.

4. Schalkoff, R.J, (1992). *Pattern Recognition – Statistical, Structural and Neural Approaches.* Singapore : John Wiley and Sons, Inc.

5. Jain, A. and Vailaya, A, (1998). Shape-Based Retrieval : A Case Study with Trademark Image Databases. *Pattern Recognition*. 31(9) : 1369-1399.

6. Jain, A.K. and Vailaya, (1995). Image Retrieval Using Colour and Shape. *Second Asian Conference on Computer Vision* (ACCV'95). II, 529-533.

7. Mukundan, R. and Ramakrishnan, K.R, (1998). *Moment Functions in Image Analysis, Theory and Applications*. Singapore : World Scientific Publishing Co.

8. Hu, M.K, (1962). Visual Pattern Recognition by Moments Invariants. *IRE Transactions on Information Theory*. 8 : 179-187.

9. Khotanzad, A and Hong, Y.H, (1990). Invariant Image Recognition by Zernike Moments. *IEEE Trans. on Pattern Analysis and Machine Intelligence*. 12(5) : 489-497.

10. Khotanzad, A. and Hong, Y.H, (1988). Rotation invariant pattern recognition using Zernike moments. *9th International Conference on Pattern Recognition*. 1, 326-328.

11. Khotanzad, A. and Lu, J.H, (1988). Distortion invariant character recognition by a multi-layer perceptron and back-propagation learning. *IEEE International Conference on Neural Networks*. 1, 625-632.

12. Khotanzad, A. and Lu, J.H, (1989). Object recognition using a neural network and invariant Zernike features. *Proceedings IEEE Computer Society Conference on Computer Vision and Pattern Recognition*, 200-205.

13. Khotanzad, A. and Lu, J.H, (1990). Classification of invariant image representations using a neural network. *IEEE Transactions on Acoustics, Speech, and Signal Processing*. 38(6) : 1028-1038.

14. Ministry of Trade and Industry Malaysia, (1995) . *Trademark Ordinance*.

15. Ministry of Trade and Industry Malaysia, (1994). *Trademark Ordinance*.

16. Otsu, N, (1979). A Threshold Selection Method from Gray Level Histogram. *IEEE Transactions on Systems Man & Cybernetics*. SMC-9 : 62-66.

17. Puteh Saad, Safaai Deris, Dzulkifli Mohamad and Habsah Abdullah, (1999). Trademark Image Registration – A Review of the Current Systems. *Jurnal Teknologi Maklumat*, FSKSM, UTM Skudai. 11(1) : 81-95.

18. Siti Mariyam Hj Shamsuddin, (2000). *Higher Order Centralised Scale-Invariants for Unconstraint Isolated Handwritten Digits*. Universiti Putra Malaysia : Ph.D. thesis.

APPENDIX A

FOUR CATEGORIES OF TRADEMARK IMAGE SAMPLES

Category 1 CIRCLE

im23 im24 im50 im51 im61


im63 im64 im69 im71 im75




Category 2 RECTANGLE

im2 im3 im4 im7 im8

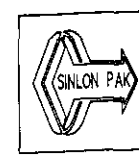

im9 im12 im40 im46 im16

APPENDIX B

Category 3 WORD-EMBEDDED

im43 im41 im80 im85 im72

im42 im47 im81 im77 im70

Category 4 COMPLEX

im17 im79 im26 im66 im88


i73 im41 im27 im28 im38